Tetrahedron 64 (2008) 7097–7105

Contents lists available at ScienceDirect

Tetrahedron

journal homepage: www.elsevier.com/locate/tet

Synthesis and metal complexation properties of bisbenzospiropyran chelators in water

Satish Kumar, Cindy Chau, Gordon Chau, Alison McCurdy *

Department of Chemistry and Biochemistry, California State University, Los Angeles, 5151 State University Drive, Los Angeles, CA 90032, USA

ARTICLE INFO

Article history:
Received 21 March 2008
Received in revised form 12 May 2008
Accepted 16 May 2008
Available online 21 May 2008

Keywords:
Metal complexation
Calcium chelator
Spiropyran
Luminescence

ABSTRACT

As a step towards developing a light-controlled reversible binding switch based on photochromic bisbenzospiropyran for investigating intracellular calcium signaling, substituted bisbenzospiropyran and phenolic chelators were synthesized and examined for metal binding strength. The complexation of these compounds with alkaline earth and zinc ions in methanol and buffer was characterized using NMR and luminescence spectroscopies. An increased length of convergent ligands on the rigid scaffold maintained binding affinity for Ca^{2+} but decreased selectivity for Ca^{2+} over Mg^{2+}. Results indicate that at least three carboxylate ligands are required for significant binding, and increased length of the ligands will result in a fully water-soluble photoswitch that exhibits two states with approximately 300-fold difference in binding affinity for Ca^{2+}.

© 2008 Elsevier Ltd. All rights reserved.

1. Introduction

Calcium ion (Ca^{2+}) is an essential signaling molecule for a number of vital cell processes, including fertilization and development.[1] This signal may act locally in small compartments of the cell or globally throughout the cell. Additionally, the concentration of Ca^{2+} may oscillate at a variety of frequencies and different durations. However, little is known about the effect of these oscillations at molecular level. A photochromic molecule that binds and releases Ca^{2+} in response to light would provide an excellent tool for understanding the effect of these oscillations on a single protein by imposing oscillations of defined frequency. Since magnesium ion (Mg^{2+}) is also present at significant concentrations in cells, the photochromic system should be selective for Ca^{2+} over Mg^{2+}. Cage compounds have been developed and reported in the literature for binding or releasing Ca^{2+} under the influence of light.[2] The main drawback in using caged calcium for mimicking an oscillatory signal is that the technique leads to irreversible decomposition of the cage, limiting the number of oscillations possible.

A number of research groups have reported photochromic compounds for binding and releasing divalent cations.[3] While these compounds show promise as photoswitchable systems, they are poorly soluble in water and are therefore less suitable for biochemical applications. To date, no fully water-soluble reversible photoswitch for binding and releasing Ca^{2+} has been demonstrated.

A photochromic bisbenzospiropyran derivative **1a** has been proposed previously as a reversible calcium cage (Fig. 1). The substituent and solvent effects on the photochromic properties of bisbenzospiropyran have been reported.[4] The metal binding affinities of three metal ions with the water-soluble compound **1a** were determined by NMR and reported in a preliminary letter.[5] Compound **1a** was found to be fairly selective for Ca^{2+} over Mg^{2+}, but the binding affinity for Ca^{2+} was not adequate for use in cellular systems, and the ability of compound **1a** to release Ca^{2+} upon irradiation was not established. Here, we report a significant extension of the preliminary study. The results of increasing the length of the ligating arm on this rigid scaffold (**1b**) as well as the effect of varying the number of chelating groups (**10a** and **10b**) on the binding affinity for Ca^{2+} and Mg^{2+} as well as other cations are presented. The use of cations with a range of atomic radii (from Mg^{2+} to Sr^{2+} or even Ba^{2+}) better allows the identification of trends

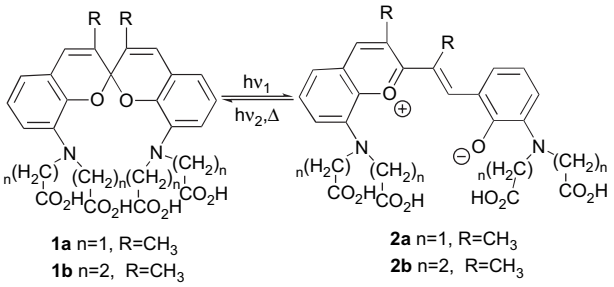

Figure 1. Forms **1** and **2** (interconvertible and photochromic if R=H).

* Corresponding author. Tel.: +1 323 343 2362; fax: +1 323 343 6490.
E-mail address: amccurd@calstatela.edu (A. McCurdy).

0040-4020/$ – see front matter © 2008 Elsevier Ltd. All rights reserved.
doi:10.1016/j.tet.2008.05.083

in binding affinity and selectivity. Additionally, to estimate the binding affinity of the short-lived open form **2** with metal ions, two control molecules possessing iminodiacetic acid and iminodipropionic acid groups (**12a** and **12b**) were also investigated. Taken together, these results establish the suitability of rigid bisbenzospiropyran derivatives as binding switches for Ca^{2+}.

2. Results and discussion

2.1. Synthesis

Chelator **1b** was obtained in four steps as shown in Scheme 1. The reaction of 3-nitrosalicylaldehyde with 3-pentanone in the presence of HCl (g) in ethanol provided 8,8′-dinitrobisbenzospiropyran **3** in excellent yield. Compound **3** was reduced with tin(II) chloride to give **4** in a good yield. Compound **4**, on reaction with ethyl bromopropionate, resulted in a workable yield of **5**. The yield of compound **5** is low, presumably due to the competing elimination reaction as well as to unfavorable sterics. Hydrolysis of **5** with aqueous NaOH in tetrahydrofuran provided target compound **1b** in good yield. Compound **1b** is soluble up to $\sim 2.5\times10^{-3}$ M in aqueous solutions buffered at pH 8.7–9.8.

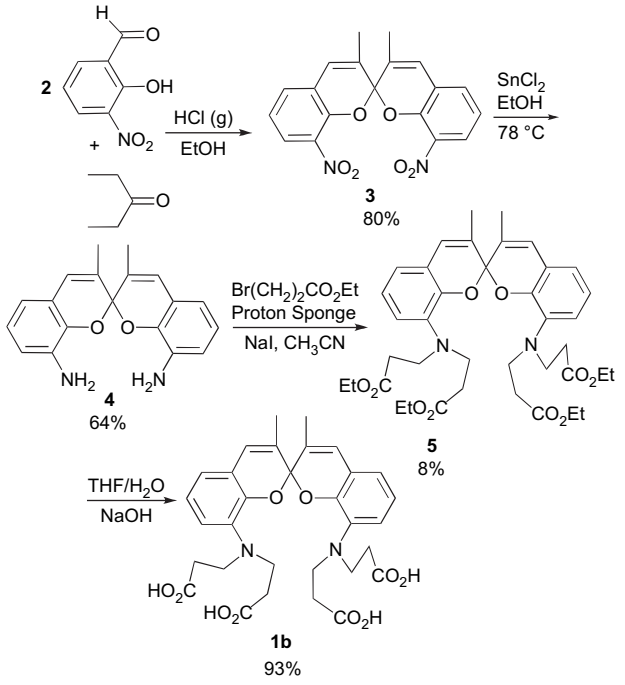

Scheme 1. Synthesis of **1b**.

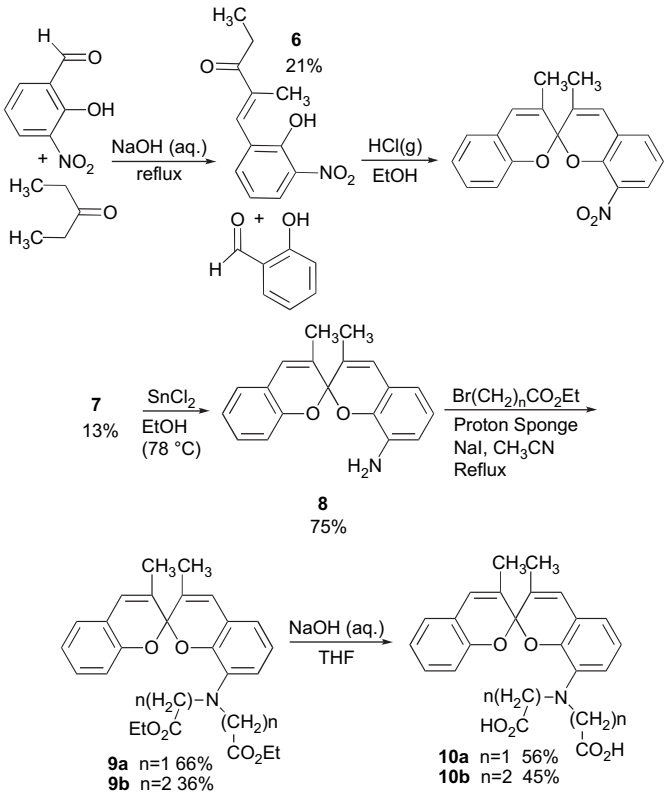

Scheme 2. Synthesis of **10a** and **10b**.

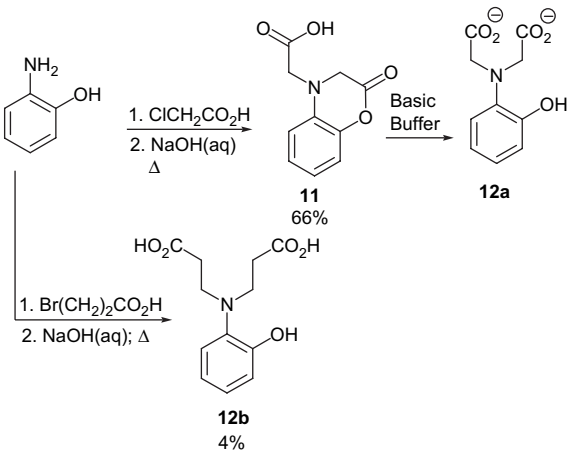

Scheme 3. Synthesis of **12a** and **12b**.

Chelators **10a** and **10b** were synthesized in five steps as shown in Scheme 2. The reaction of 3-nitrosalicylaldehyde with 3-pentanone under basic conditions provided compound **6** in moderate yield, which on reaction with salicylaldehyde in ethanol in the presence of HCl gave asymmetric 8-nitrobisbenzospiropyran (**7**). Compound **7** was converted to chelators **10a** and **10b** through reduction, addition of acetate or propionate groups, and hydrolysis.

Chelator **12a** was synthesized as a lactone **11** by reaction of chloroacetic acid with *o*-aminophenol in the presence of aqueous sodium hydroxide in good yield as described in the literature.[6] Compound **11** converts quantitatively to **12a** in basic buffer, confirmed by ^{1}H NMR and ^{13}C NMR. Chelator **12b** was synthesized by reacting bromopropionic acid with 2-aminophenol in the presence of aqueous base (Scheme 3). The yield was low due to the competing elimination reaction.

2.2. Metal complexation studies

2.2.1. Determination of binding affinity by NMR

NMR, UV, and luminescence spectroscopies have been used extensively to determine binding affinities.[7] Due to the very small changes in the UV absorption spectra on addition of metal ions to **1b**, **10a**, and **10b**, UV–vis spectroscopy was not used for binding constant determinations here. ^{1}H NMR titrations were performed to obtain binding affinities (K_a) and maximum complexation induced shifts ($\Delta\delta_{max}$) for chelators **1b**, **10a**, **10b**, **12a**, and **12b** with metal ions, as has been reported earlier for **1a**.[5] All the equilibria considered in fitting the data are shown in Figure 2. Figure 3 shows an example of the experimental values and the calculated values of the best fit binding model (1:1 binding only) for titration of Ca^{2+} with chelator **12a**.

$$\text{chelator} + M^{2+} \rightleftharpoons \text{chelator}M^{2+} \quad K_{11}$$
$$\text{chelator} + 2M^{2+} \rightleftharpoons \text{chelator}(M^{2+})_2 \quad K_{12}$$
$$2\text{chelator} + M^{2+} \rightleftharpoons (\text{chelator})_2M^{2+} \quad K_{21}$$

Figure 2. Simultaneous binding equilibria considered in modeling ^{1}H NMR and luminescence titration data of chelators **1a**, **1b**, **10a**, **10b**, **12a**, and **12b**.

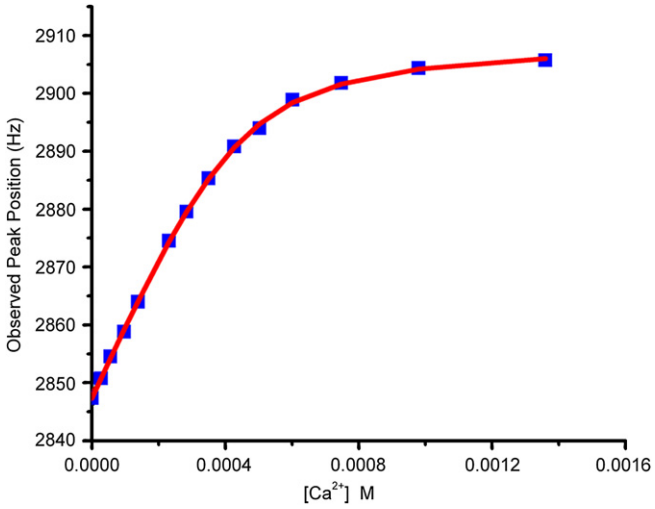

Figure 3. Observed ^{1}H NMR peak position (■) and calculated peak position (—) for one aromatic proton of **12a** during a titration with $CaCl_2$ (aq) in HEPES buffer (10 mM, pH=9.8); $[\mathbf{12a}]_0=4.6\times10^{-4}$ M, $[Ca^{2+}]=0$–1.36×10^{-3} M.

The results of all ^{1}H NMR binding titrations using the best fit binding models are shown in Table 1. A significant but small change in NMR chemical shift was observed for **10a**, **12a**, and **12b** on addition of metal ions. The change in chemical shift on addition of metal ion was very small for **1b** (~5 Hz), however, leading to inaccurate results (Supplementary data). For **10b**, the observed change in chemical shift was in the range 7–10 Hz on a 600 MHz instrument, but did not reach saturation, especially with Sr^{2+}. Therefore, the binding affinity of metals to **10b** was considered to be negligible under these conditions. ^{1}H NMR titration was not an appropriate technique for quantitative determination of binding affinities for both **1b** and **10b**.

The binding affinities (K_{11}) of **10a** were small, but stronger than those of **10b**, and were in the order $Ca^{2+}>Mg^{2+}\gg Sr^{2+}$. The overall stability constant K_{21} divided by K_{11} gives the affinity of a second chelator **10a** to the 1:1 complex, which in this case is relatively large for all three metals. Presumably this additional equilibrium is significant for this chelator because the metals are incompletely coordinated, due to **10a** having the fewest coordinating atoms of all the chelators studied. The binding affinities of **12a** were stronger than those of **12b** and were in the order $Ca^{2+}>Mg^{2+}>Sr^{2+}$. This is in agreement with the binding constants for **12a** that have been reported previously in 0.1 M KNO_3 (1:1 binding model, by potentiometry).[6] For **12b**, the binding affinities followed the order $Mg^{2+}>Ca^{2+}>Sr^{2+}$. The increase of selectivity for smaller metal ions with increasing chelate ring size has been well established in the literature.[8] According to the best fit binding model, the affinity of a second chelator **12b** to the 1:1 complex is significant for complexes of Ca^{2+} and Sr^{2+}, while there is no significant additional equilibrium for **12b** and Mg^{2+}, or for **12a** and any metal ion studied. The additional equilibrium for **12b** and Ca^{2+} and Sr^{2+} suggests that these larger metal ions, when associated with **12b**, remain available for additional coordination. Overall, shorter ligating arms bind Ca^{2+} preferentially, while longer ligating arms bind the smaller Mg^{2+} preferentially. Additionally, larger metals bound weakly to chelators **10** and **12** may participate in additional relatively significant binding equilibria with a second chelator.

Table 1
Best fit binding constants (K_{11} and K_{21}) and maximum shifts of α hydrogens ($\Delta\delta_{max}$) for chelators **10a**, **10b**, **12a**, and **12b** in 10 mM HEPES pH 9.8 by ^{1}H NMR[a]

		K_{11} (M^{-1})	K_{21} (M^{-2})	K_{21}/K_{11} (M^{-1})	$\Delta\delta_{max}$ (Hz)[b]
10a	Mg^{2+}	$5.98\pm0.72\times10^{0}$	$1.47\pm0.57\times10^{5}$	$2.53\pm1.22\times10^{4}$	24.5
	Ca^{2+}	$1.55\pm0.12\times10^{1}$	$5.31\pm2.8\times10^{4}$	$3.50\pm2.07\times10^{3}$	22.7
	Sr^{2+}	$8.0\pm1\times10^{-2}$	$6.88\pm1.24\times10^{4}$	$8.13\pm1.18\times10^{5}$	283.5
10b	Mg^{2+}, Ca^{2+}, Sr^{2+}	Negligible			7–10 (obs)
12a	Mg^{2+}	$3.28\pm0.18\times10^{3}$	$4.87\pm0.58\times10^{2}$	$1.50\pm0.24\times10^{0}$	31.3
	Ca^{2+}	$1.57\pm0.28\times10^{4}$	$1.80\pm0.35\times10^{5}$	$1.14\pm0.13\times10^{1}$	51.1
	Sr^{2+}	$7.58\pm0.95\times10^{2}$	$8.93\pm1.19\times10^{2}$	$1.19\pm0.17\times10^{1}$	34.5
12b	Mg^{2+}	$2.66\pm0.46\times10^{2}$	$3.87\pm0.62\times10^{3}$	$1.46\pm0.09\times10^{1}$	32.6
	Ca^{2+}	$1.71\pm0.15\times10^{1}$	$5.19\pm0.98\times10^{4}$	$3.02\pm0.28\times10^{3}$	12.8
	Sr^{2+}	$9.0\pm1\times10^{-2}$	$2.16\pm0.83\times10^{4}$	$2.32\pm0.49\times10^{5}$	493.2

[a] Average of at least three trials; $[\text{chelator}]=2\times10^{-4}$ M; $[M^{2+}]=0$–0.3 M for **10a**, **10b**, and **12b** and 0–0.03 M for **12a**.
[b] Frequency: 600 MHz spectrometer for **10a** and **10b**; 400 MHz spectrometer for **12a** and **12b**.

2.2.2. Determination of binding affinity by luminescence

To obtain reliable binding affinities for **1b** and **10b**, a spectroscopic technique with larger observable changes upon metal binding is required. Therefore, luminescence characteristics of **1b** and **10b** were examined in methanol and HEPES buffer (10 mM, pH=9.8). While aqueous buffer simulates physiological conditions, methanol was also used so the effects of the protonation state on luminescence could be determined. Luminescence of compounds **1a** and **10a** was also examined for comparison. Absorption and luminescence spectra in methanol and HEPES buffer (10 mM, pH=9.8) for these compounds are provided in Supplementary data.

The luminescence changes observed for **1b** were surprising, and were explored more quantitatively to determine the utility of these compounds as fluorescent cation sensors. Therefore, quantum yields of compounds **1a** and **1b** were determined in methanol and HEPES buffer (10 mM, pH=9.8) using Eaton's method (Table 2).[9] The magnitude of the quantum yields for these compounds is similar to those reported for the luminescence of spiroindolinopyrans.[10] The quantum yield of **1a** was lower than that of **1b** in both solvent systems. The quantum yield of **1b** was higher in methanol than in HEPES buffer, while the quantum yield of **1a** was lower in methanol than in HEPES buffer. This may be due to quenching of luminescence of **1a** in methanol by dissolved oxygen, as the viscosity of aqueous buffer solution is higher than that of methanol. This behavior is consistent with a longer luminescence lifetime for **1a** than that for **1b**.[9c,d]

2.2.2.1. Effects of cations on luminescence. The effects of protonation state on luminescence behavior of **1a** and **1b** in methanol were complex. For **1a**, full deprotonation by addition of methoxide significantly increased emission, and full protonation by addition of trifluoroacetic acid (or toluenesulfonic acid) also increased emission. For **1b**, addition of methoxide increased emission, but addition of acid decreased it (Supplementary data). The dissimilar luminescence behavior of **1a** and **1b** may be attributed to

Table 2
Quantum yields for **1a** and **1b** with respect to anthracene

Compound	λ_{ex} (nm)	Solvent	Quantum yield
1a	310	HEPES buffer (10 mM, pH=9.8)	0.0057±0.0006
1a	310	Methanol	0.0034±0.0002
1b	310	HEPES buffer (10 mM, pH=9.8)	0.0083±0.0005
1b	315	HEPES buffer (10 mM, pH=9.8)	0.0071±0.0002
1b	310	Methanol	0.027±0.0007

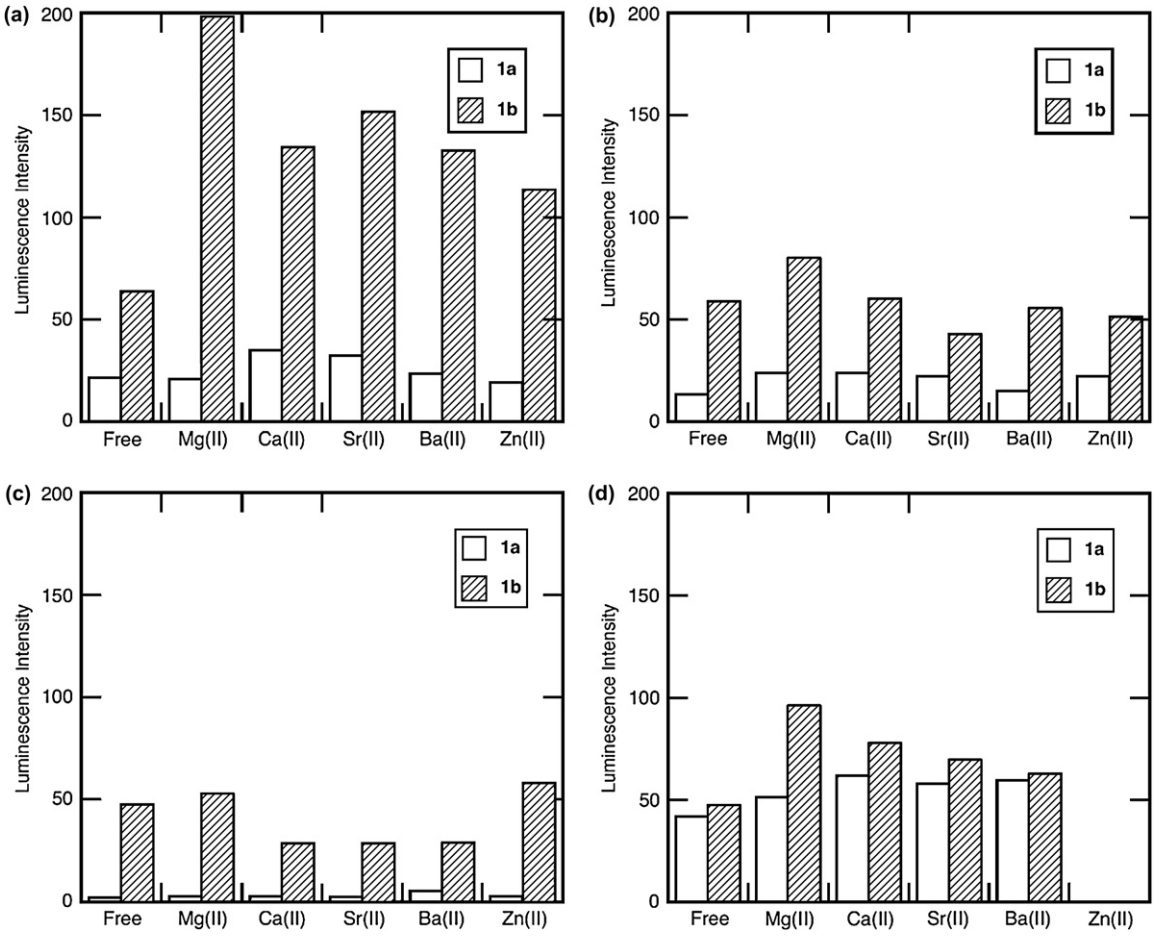

Figure 4. Luminescence intensity at λ_{max} on addition of metal chloride to **1a** (unshaded) and **1b** (shaded) (a) in methanol after purging the solution with argon; (b) in methanol under ambient conditions; (c) in methanol after purging with oxygen (99.95%): [**1a**]=6×10^{-6} M; [**1b**]=2×10^{-6} M; [M^{2+}]≈0.05 M; (d) in 10 mM HEPES pH 9.8 under ambient conditions: [**1a**]=2.3×10^{-5} M; [**1b**]=2.7×10^{-5} M; [M^{2+}]=0.03 M. Spectra were corrected for dilution.

differences in intramolecular H-bonding or inductive effects, and were not explored further.

The changes in intensity of luminescence spectra of **1a** and **1b** on addition of a variety of metal ions were examined in methanol. Luminescence intensity of both **1a** and **1b** increased on addition of metal ions. In the case of **1b** in methanol, the addition of metal ions did not have the same effect as the addition of acid. Therefore, the effect of metal binding on luminescence properties of **1b** was not simply electrostatic. In addition, the UV absorbance spectra in the presence and absence of metal ions did not reveal any changes in the degree of conjugation or in absorbance (Supplementary data). Therefore, conformational restrictions upon metal chelation may play a role in the luminescence changes upon metal binding for **1b** in methanol.[11] Under binding saturation conditions, the largest increase in relative luminescence intensity of **1b** in methanol occurred with the addition of Mg^{2+}, while for **1a** it occurred with the addition of Ca^{2+} (Fig. 4 and Supplementary data). The addition of Zn^{2+}, a metal ion known to bind strongly to carboxylate ligands, also resulted in an increase in luminescence intensity for **1b**, and less for **1a**.

A comparison of luminescence intensity while purging with argon, under ambient conditions, and purging with oxygen showed that oxygen quenched luminescence (Fig. 4a–c). Luminescence of **1a** was more sensitive to quenching by oxygen in comparison to **1b**. These data suggest that **1a** has a longer-lived excited state than **1b**.[9c,d]

Luminescence intensity of **10a** in methanol did not change significantly upon addition of metal ion, however, the luminescence of **10b** did change significantly (Fig. 5). Addition of Zn^{2+} to **10b** in methanol under ambient conditions resulted in an 18-fold increase in intensity of luminescence. As for **1a** and **1b**, the luminescence of **10a** and **10b** increased on purging the solution with argon (Fig. 5).

Luminescence studies of **1a**, **1b**, **10a**, and **10b** were also performed in HEPES buffer (10 mM, pH=9.8). The effects of protonation state could not be pursued in aqueous buffer, for the protonated chelators were insoluble. The addition of Zn^{2+} in aqueous basic buffer was not pursued due to its low solubility. There was only a small luminescence enhancement upon metal addition for chelators **1a** and **10a**, so luminescence binding studies were not pursued for these compounds. Figure 4d shows the change in emission intensity of **1a** and **1b** upon addition of metal ions in aqueous basic buffered solution. The luminescence spectrum of **1b** showed significant enhancement of intensity as well as dramatic shifting to shorter wavelengths on addition of Ca^{2+} and Mg^{2+}, as shown in Figure 6, but very little change on addition of Sr^{2+}. As in methanol, in buffer the largest relative increase in intensity of luminescence for **1b** occurred with Mg^{2+} and with Ca^{2+} for **1a**. The luminescence spectrum of **10b** showed enhancement of intensity on addition of metal ions (Ca^{2+} and Mg^{2+}) but there was no shift in the λ_{max} of luminescence (Supplementary data). For **10b**, Sr^{2+} had no effect on fluorescence, while addition of Ba^{2+} decreased the intensity. The intensity of luminescence of **1b** in HEPES buffer (10 mM, pH=9.8) did not change on purging with oxygen (Supplementary data). Given the significant changes in luminescence spectra upon addition of metal ion, monitoring luminescence changes should allow the determination of metal binding affinities for **1b** and **10b**.

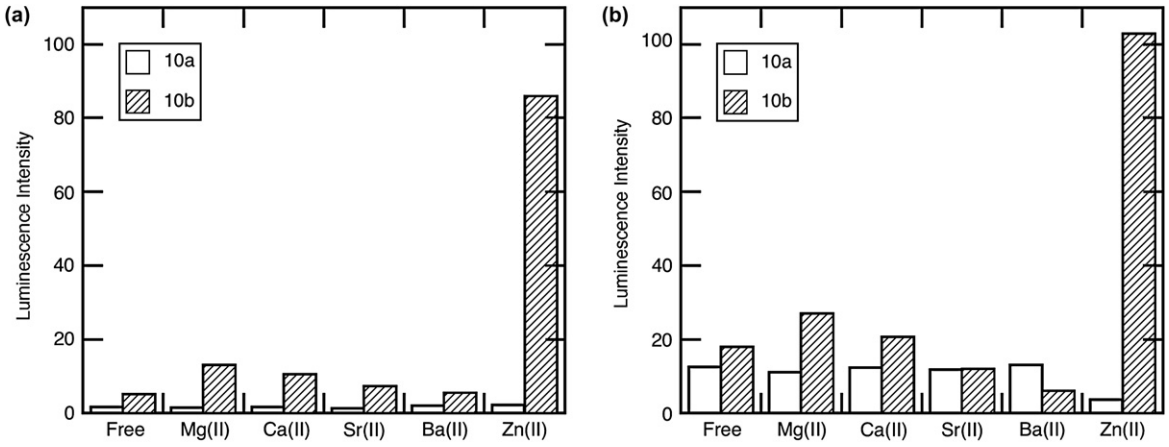

Figure 5. Luminescence intensity at λ_{max} on addition of metal chloride to **10a** (unshaded) and **10b** (shaded) in methanol (a) under ambient conditions; (b) after purging with argon: [**10a**]=1.9×10^{-5} M; [**10b**]=2.2×10^{-5} M; [M^{2+}]≈0.05 M. Spectra were corrected for dilution.

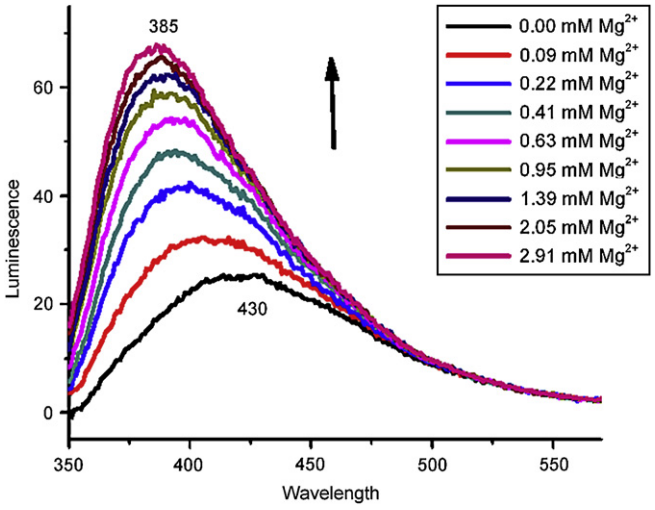

Figure 6. Luminescence intensity of **1b** ([**1b**]$_0$=3.27×10^{-5} M, λ_{ex}=315 nm) on addition of $MgCl_2$ in HEPES buffer (10 mM, pH=9.8). Spectra are corrected for dilution.

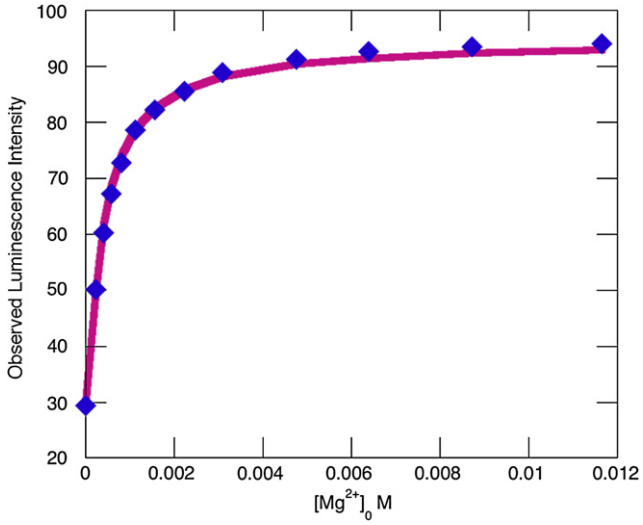

Figure 7. Observed luminescence intensity (■) and calculated luminescence intensity (—) of **1b** during a titration with $MgCl_2$ (aq) in HEPES buffer (10 mM, pH=9.8). Data are corrected for dilution; [**1b**]$_0$=2.37×10^{-5} M.

2.2.2.2. Analysis of luminescence titration data. Hyperquad 2006[12] was used to obtain the best fit binding constants for **1b** and **10b** using luminescence data in HEPES buffer (10 mM, pH=9.8). For **1b** and Mg^{2+} or Sr^{2+}, the use of a single equilibrium (K_{11}) resulted in the best fit to the observed data as shown in Figure 7. The use of additional equilibria did not improve the fit. For **1b** and Ca^{2+}, two equilibria (K_{11} and K_{12}) resulted in the best fit. Table 3 shows the best fit binding association constants determined from luminescence data for **1b**.

For **1b**, monitoring luminescence changes upon metal binding has allowed an accurate determination of binding constants. The binding affinities were in the order Ca^{2+}>Mg^{2+}>Sr^{2+}, and this chelator is slightly selective for Ca^{2+} over Mg^{2+}. The overall stability constant K_{12} divided by K_{11} gives the affinity of a second Ca^{2+} to the 1:1 complex, which in this case is small (135±50 M^{-1}). Since the data did not fit to an additional K_{21} equilibrium, Ca^{2+} is more fully encapsulated by **1b**, compared to chelators **10** and **12**, with fewer coordinating ligands. For **10b**, however, luminescence titration did not offer improved binding constant determinations compared to NMR, despite a larger signal to measure (Supplementary data). This is presumably due to the weakness of binding and inability to reach saturation during the binding titration. Qualitatively, **10b** binds Ca^{2+}, Mg^{2+}, and Sr^{2+} very weakly.

2.3. Suitability of scaffolds 1a and 1b as binding switches

Comparing previously determined binding affinities of **1a** for Ca^{2+} and Mg^{2+} in Table 4 to those determined here of **1b** suggests that increasing the length of the ligands by one additional methylene group resulted in only a slight decrease in binding affinity for Ca^{2+}. In turn, there was a relative increase in affinity for Mg^{2+}. Therefore, for **1b** the entropic penalty of binding with longer, flexible ligands must be compensated by favorable enthalpy by closer interaction with the cation, especially for the smaller Mg^{2+} cation.[13] Both closed forms **1a** and **1b** bind Ca^{2+} moderately well, but **1b** is less selective for Ca^{2+} than **1a**. The absence of an additional significant K_{21} equilibrium with Ca^{2+} for **1b**, which was observed for **1a**, suggests that Ca^{2+} bound to **1b** is more effectively surrounded by ligands than if it were bound to **1a**.

In the absence of crystal structures, compounds **10a** and **10b** were designed to better understand the features required for alkaline earth metal binding to this rigid bisbenzospiropyran scaffold. Comparison of binding affinities of **1a** and **10a** (or **1b** and **10b**) confirms that three or more carboxylate groups are required for the significant binding of Ca^{2+} and Mg^{2+} observed for **1a** and **1b**. Therefore, the two perpendicular sets of iminodiacetic or

Table 3
Best fit binding constants (K_{11} and K_{12}) for **1b** in HEPES buffer (10 mM, pH=9.8) by luminescence spectroscopy[a]

		K_{11} (M^{-1})	K_{12} (M^{-2})	K_{12}/K_{11} (M^{-1})
1b	Mg^{2+}	$3.66\pm0.25\times10^3$	$7.56\pm3.0\times10^5$	$1.34\pm0.50\times10^2$
	Ca^{2+}	$5.60\pm0.67\times10^3$		
	Sr^{2+}	$3.59\pm0.16\times10^2$		

[a] Average of at least three trials; $[\mathbf{1b}]_0=3\times10^{-5}$ M; $[M^{2+}]$=0–0.03 M.

Table 4
Best fit binding constants (K_{11}, K_{12}, and K_{21}) for **1a** in HEPES buffer (10 mM, pH=9.8) by ^{1}H NMR spectroscopy[5]

		K_{11} (M^{-1})	K_{12} (M^{-2})	K_{21} (M^{-2})
1a	Mg^{2+}	5.64×10^2	2.87×10^1	2.11×10^6
	Ca^{2+}	6.72×10^3	5.10×10^5	4.41×10^7

iminodipropionic acid groups are convergent and do not effectively bind metals at two independent sites. This interpretation is supported by the results that the affinity for the **1**–M^{2+} complex for a second metal ranged from 0 to only 135 M^{-1}.

The short-lived open form **2** of bisbenzospiropyran prevents the determination of binding affinities directly. Instead, model compounds were used to estimate the binding affinity of the open forms **2a** and **2b**. If the zwitterionic resonance structure of **2** is a major resonance contributor in buffer, only one of the two possible binding sites should have appreciable affinity for metal ions. The iminodiacetic or iminodipropionic acid group of **2a** or **2b** that is located on the electron-deficient ring was neglected as a binding site for metal ions. This assumption is supported by the observed low affinity of **10a** and **10b** for metal ions. The electron deficiency of the positively charged ring in the zwitterionic form of **2** would presumably give rise to an even smaller affinity than those of compounds **10**. Therefore, compounds **12a** and **12b** were chosen to serve as adequate binding site models for open forms **2a** and **2b**.

A comparison of affinities of **1a** and **12a** (a mimic of **2a**) suggests that form **2a** would not release Ca^{2+} more readily than **1a**, and that the form **2a** would be selective for Ca^{2+} over Mg^{2+}. Comparison of affinities of **1b** and **12b** (a mimic of **2b**) suggests that form **2b** would release Ca^{2+} much more readily than **1b**, with a possible 330-fold binding affinity difference between the two forms. In addition, form **2b** would be selective for Mg^{2+} over Ca^{2+}. Therefore, **1b** shows promise as a superior photoswitch in binding affinity relative to **1a**. However, in a biological context in which both Ca^{2+} and $Mg^{2+}$are present, Mg^{2+} would interfere more when using **1b** as a binding photoswitch than when using **1a**.

3. Conclusion

NMR and luminescence of bisbenzospiropyran derivatives and related model compounds have been used in this work to determine binding affinities for metal ions, including Ca^{2+} and Mg^{2+}. Results of this research will be used in the design of a reversible cage for calcium triggered by light. Structural modifications to the bisbenzospiropyran scaffold will be required to improve the photophysical properties of the binding photoswitch. Further work in this direction is in progress.

4. Experimental

4.1. General methods

Flash column chromatography was performed using Silica Gel 60 (230–400 mesh). ^{1}H NMR and ^{13}C NMR spectra were recorded on a 300 MHz Bruker Aspect 3000 spectrometer and 400 MHz Bruker Avance II spectrometer at ambient temperature. Chemical shifts are reported in parts per million relative to residual solvent signal or TMS. High resolution mass spectra were obtained at the University of California at Riverside Mass Spectroscopy Facility. UV–vis spectra were recorded on a Cary 50 Bio UV–visible spectrometer. IR spectra were recorded on a Themo Nicolet 6700 FT-IR spectrometer in KBr pallet. Yields refer to chromatographically and spectroscopically pure materials, unless otherwise stated. Salicaldehyde (98%), acetonitrile (anhydrous), ethanol (anhydrous), 2-aminophenol, chloroacetic acid, 3-bromopropionic acid, ethyl bromoacetate, ethyl bromopropionate, 3-pentanone, proton sponge™, 2-hydroxy-3-nitrobenzaldehyde, $SnCl_2\cdot2H_2O$, $MgCl_2$ (anhydrous), $CaCl_2$ (anhydrous), $SrCl_2$ (anhydrous), and $ZnCl_2$ (anhydrous) were obtained from Aldrich. NaI was obtained from Spectrum. HEPES-d_{18} was obtained from Cambridge Isotope Laboratories, Inc. Synthesis of compounds **3**, **4**, and **1a** have been reported previously.[5]

*4.1.1. 3,3′-Dimethyl-8,8′-bis(diethyl iminopropanoate)-2,2′-spirobi[2H-1-benzopyran] (**5**)*

To a stirred solution of compound **3** (0.34 g, 1.11 mmol) in 30 mL anhydrous acetonitrile in a 100 mL three-neck round bottom flask equipped with a condenser were added sodium iodide (0.02 g, 0.13 mmol), Proton Sponge™ (2.08 g, 9.74 mmol), and ethyl bromopropionate (1.1 mL, 8.62 mmol). The reaction mixture was refluxed under N_2 atmosphere for 48 h.[5] Reaction progress was monitored by TLC using 5% ethyl acetate in methylene chloride as solvent. The reaction mixture was diluted with toluene, filtered, and the precipitate was washed with toluene. The combined toluene portions were washed several times with pH 2 phosphate buffer and water, dried over magnesium sulfate, filtered, and evaporated under reduced pressure. The crude product was purified by flash chromatography (5% ethyl acetate in methylene chloride) to give **5** (62.7 mg, 8%). IR (KBr pallet, ν/cm^{-1}): 1732. ^{1}H NMR ($CDCl_3$, 300 MHz, δ): 6.86–6.72 (m, 8H), 6.66 (d, J=1.2 Hz, 2H), 4.02 (q, J=7.2 Hz, 8H), 3.21 (t, J=7.3 Hz, 8H), 2.30 (t, J=7.3 Hz, 8H), 1.94 (d, J=1.0 Hz, 6H), 1.18 (t, J=7.20 Hz, 12H). ^{13}C NMR (75 MHz, $CDCl_3$, δ): 172.5, 143.7, 137.2, 128.8, 124.0, 121.9, 121.3, 120.9, 120.4, 102.2, 60.3, 48.8, 33.7, 18.6, 14.4. HRMS (m/z): calcd (MH^+) 707.3544; found 707.3569.

*4.1.2. 3,3′-Dimethyl-8,8′-bis(iminodipropanoic acid)-2,2′-spirobi[2H-1-benzopyran] (**1b**)*

To a stirred solution of compound **5** (11.8 mg, 1.67×10^{-5} mol) in 1 mL of tetrahydrofuran (THF) in a 5 mL point bottom flask was added 40 μL of 2.5 M NaOH (1×10^{-4} mol). The reaction mixture was stirred at room temperature for 96 h. Reaction progress was monitored by reverse-phase TLC (20% CH_3CN in water), and occasionally few drops of water were added. After 48 h, 20 μL of 2.5 M NaOH (5×10^{-5} mol) was added to the reaction mixture. The sample was lyophilized. The crude sample was then acidified with 6 M HCl and dissolved in a minimum of acetonitrile before being applied to a 6 mL SPE tube (Supelco Supelclean™ LC-18). Stepwise gradient elution using 10%, 20%, and 30% acetonitrile in water was used to isolate the pure product **1b** (9.2 mg, 92.7%). IR (KBr pallet, ν/cm^{-1}): 3426, 2558, 1716. ^{1}H NMR (acetone-d_6, 400 MHz, δ): 6.96–6.90 (m, 6H), 6.69 (d, J=1.4 Hz, 2H), 3.25–3.30 (m, 8H), 2.34 (t, J=7.2 Hz, 8H), 1.97 (d, J=1.4 Hz). ^{13}C NMR (75 MHz, acetone-d_6, δ): 172.5, 143.9, 136.2, 128.6, 123.7, 122.2, 121.3, 121.3, 120.9, 102.4, 48.6, 32.1, 17.6. HRMS (m/z): calcd 595.2292 (M^+); found 595.2270.

*4.1.3. 1-(2-Hydroxy-3-nitrophenyl)-2-methyl-pent-1-ene-3-one (**6**)*

To a 50 mL flask equipped with a condenser were added 2-hydroxy-3-nitrobenzaldehyde (1.00 g, 6.04 mmol), 4 N NaOH (aq) (6.0 mL, 24 mmol), and pentanone (6.5 mL, 61.3 mmol). The mixture was stirred and refluxed overnight. The reaction progress was

monitored by TLC (30% ethyl acetate in hexane). After 24 h, the reaction was stopped, cooled to room temperature, neutralized with 5% HCl, and extracted several times with ethyl acetate. The organic layer was washed with water and dried over magnesium sulfate, filtered, and evaporated under reduced pressure. The crude product was purified by column chromatography (10% ethyl acetate: 90% hexane) to give pure **6** (0.29 g, 21%). IR (KBr pallet, ν/cm^{-1}): 3248, 1694. ^{1}H NMR (400 MHz, $CDCl_3$, δ): 11.05 (s, 1H), 8.10 (dd, J=8.0 Hz, 1H), 7.64 (br s, 1H), 7.62 (dd, J=8.0 Hz, 1H), 7.04 (t, J=8.0 Hz, 1H), 2.87 (q, J=7.2 Hz, 2H), 1.98 (d, J=1.4 Hz, 3H), 1.17 (t, J=7.2 Hz, 3H). ^{13}C NMR ($CDCl_3$, 100 MHz, δ): 202.5, 153.2, 139.2, 137.8, 133.8, 130.9, 127.7, 125.0, 119.4, 30.9, 13.4, 8.7. HRMS (m/z): calcd 235.0845; found 235.0846.

4.1.4. 3,3′-Dimethyl-8-nitro-2,2′-spirobi[2H-1-benzopyran] (**7**)

To a solution of compound **6** (1.0 g, 4.29 mmol) in ethanol (25 mL) in a 50 mL three-neck round bottom flask was added salicylaldehyde (2.5 mL, 0.023 mol). The reaction mixture was stirred at room temperature for 72 h with periodic bubbling of dry HCl (g). The reaction progress was monitored with TLC (60% toluene in hexane). The reaction was poured over ice water and neutralized with 1 M NaOH (aq). The neutralized crude product was extracted several times with ethyl acetate. The organic layer was washed with water, dried over magnesium sulfate, filtered, and evaporated under reduced pressure. The crude product was purified by column chromatography (40% toluene/60% hexane) to give pure compound **7** (0.18 g, 13%). IR (KBr pallet, ν/cm^{-1}): 1530. ^{1}H NMR (400 MHz, $CDCl_3$, δ): 7.72 (d, J=8.2 Hz, 1H), 7.31 (d, J=7.52 Hz, 1H), 7.18–7.71 (m, 2H), 7.02–6.96 (m, 2H), 6.82 (d, J=8.2 Hz, 1H), 6.64–6.64 (m, 2H), 1.98 (dd, J=12.3 Hz). ^{13}C NMR (100 MHz, $CDCl_3$, δ): 149.6, 144.0, 138.2, 131.3, 130.2, 129.0, 127.2, 126.2, 124.5, 124.3, 122.5, 122.1, 122.0, 120.5, 119.4, 115.6, 102.8, 18.5, 18.4. HRMS (m/z): calcd 321.1001; found 321.0999.

4.1.5. 3,3′-Dimethyl-8-amino-2,2′-spirobi[2H-1-benzopyran] (**8**)

To a solution of compound **7** (0.63 g, 1.96 mmol) in ethanol (40 mL) in a 50 mL round bottom flask equipped with a condenser was added $SnCl_2 \cdot 2H_2O$ (2.21 g, 9.83 mmol). The system was evacuated and filled with N_2 gas several times, and then heated to 78 °C for 3.5 h. The reaction progress was monitored by TLC. The mixture was cooled to room temperature and neutralized with 5% $NaHCO_3$. The organic layer was extracted several times with ethyl acetate, dried over magnesium sulfate, filtered, and evaporated under reduced pressure to provide compound **8** (crude, 0.43 g, 75.4%), which was used without further purification. ^{1}H NMR ($CDCl_3$, 300 MHz, δ): 7.18–7.09 (m, 2H), 6.95 (t, J=7.5 Hz, 1H), 6.85 (d, J=8.0 Hz, 1H), 6.78 (t, J=7.5 Hz, 1H), 6.64–6.55 (m, 4H), 3.57 (br s, 2H), 1.95 (d, J=4.0 Hz, 6H). ^{13}C NMR (75 MHz, $CDCl_3$, δ): 150.2, 137.5, 134.5, 129.2, 128.8, 128.6, 125.92, 123.7, 123.3, 121.6, 121.5, 119.9, 119.5, 116.0, 115.5, 102.3, 18.7, 18.6. HRMS (m/z): calcd 291.1295; found 291.1266.

4.1.6. 3,3′-Dimethyl-8-(diethyl iminodiacetate)-2,2′-spirobi[2H-1-benzopyran] (**9a**)

To a solution of compound **8** (0.38 g, 1.32 mmol) in anhydrous acetonitrile (50 mL) in a 100 mL round bottom flask equipped with a condenser were added NaI (0.01 g, 0.66 mmol), Proton Sponge™ (0.92 g, 4.29 mmol), and ethyl bromoacetate (0.6 mL, 2.25 mmol). The system was evacuated and filled with N_2 gas. The reaction mixture was refluxed and progress was monitored by TLC (20% ethyl acetate in hexane). After 48 h, the reaction mixture was cooled to room temperature. The reaction mixture was diluted with toluene, filtered, and the precipitate was washed with toluene. The combined toluene portions were washed several times with pH 2 phosphate buffer, water, dried over magnesium sulfate, filtered, and evaporated under reduced pressure. The crude product was purified by column chromatography (14% ethyl acetate/86% hexane) to give pure **9a** (0.40 g, 66%). IR (KBr pallet, ν/cm^{-1}): 1748. ^{1}H NMR (400 MHz, $CDCl_3$, δ): 7.13 (t, J=8.0 Hz, 1H), 7.06 (d, J=7.4 Hz, 1H), 6.93 (t, J=7.4 Hz, 1H), 6.86–6.80 (m, 2H), 6.71–6.65 (m, 2H), 6.54–6.51 (m, 2H), 4.10–3.91 (m, 8H), 1.92 (dd, J=1.3 Hz, 6H), 1.17–1.13 (t, J=7.2 Hz, 6H). ^{13}C NMR (100 MHz, $CDCl_3$, δ): 171.3, 150.3, 140.3, 137.6, 128.8, 128.7, 128.6, 125.8, 123.3, 121.5, 121.4, 120.9, 119.6, 119.0, 117.9, 115.5, 102.3, 60.5, 53.6, 18.8, 18.3, 14.1. HRMS (m/z): calcd 463.1995; found 463.1990.

4.1.7. 3,3′-Dimethyl-8-(iminodiacetic acid)-2,2′-spirobi[2H-1-benzopyran] (**10a**)

To a solution of compound **9a** (52 mg, 0.0231 mmol) in tetrahydrofuran (1 mL) in a 5 mL flask was added 40 μL of 4 N NaOH (aq) (0.0924 mmol). The reaction mixture was stirred at room temperature and monitored with reverse-phase TLC. Small portions of distilled water were added over 120 h. The sample was lyophilized. The crude sample was then acidified with 6 M HCl and dissolved in a minimum of acetonitrile before being applied to a 6 mL SPE tube (Supelco Supelclean™ LC-18). Stepwise gradient elution using 10%, 20%, 30%, and 40% acetonitrile in water was used to isolate the pure product **10a** (25.8 mg, 56%). IR (KBr pallet, ν/cm^{-1}): 3420, 2635, 1721. ^{1}H NMR (400 MHz, CD_3CN, δ): 7.15 (t, J=7.4 Hz, 2H), 6.99–6.89 (m, 2H), 6.84–6.82 (m, 2H), 6.73 (d, J=8.0 Hz, 1H), 6.67 (s, 1H), 6.63 (s, 1H), 3.38 (s, 4H), 1.91 (d, J=1.1 Hz, 6H). ^{13}C NMR (400 MHz, CD_3CN, δ): 172.8, 150.0, 140.6, 136.4, 129.5, 128.8, 128.2, 126.3, 123.8, 123.0, 121.8, 121.7, 121.3, 120.0, 118.5, 114.9, 102.3, 55.1, 17.8, 17.4. HRMS (m/z): calcd 408.1447 (MH^+); found 408.1459.

4.1.8. 3,3′-Dimethyl-8-(diethyl iminodipropanoate)-2,2′-spirobi[2H-1-benzopyran] (**9b**)

To a solution of compound **8** (0.43 g, 1.47 mmol) in anhydrous acetonitrile (40 mL) in a 100 mL round bottom flask equipped with a condenser were added NaI (0.12 g, 0.8 mmol), Proton Sponge™ (1.51 g, 7.04 mmol), and ethyl bromoacetate (0.8 mL, 6.62 mmol). The system was evacuated and filled with N_2 gas. The reaction mixture was refluxed and progress was monitored by TLC (20% ethyl acetate in hexane). After 48 h, reaction mixture was cooled to room temperature. The mixture was diluted with toluene, filtered, and the precipitate was washed with toluene. The combined toluene portions were washed several times with pH 2 phosphate buffer and water, dried over magnesium sulfate, filtered, and evaporated under reduced pressure. The crude product was purified by column chromatography (14% ethyl acetate/86% hexane) to give compound **9b** (0.23 g, 36.1%). IR (KBr pallet, ν/cm^{-1}): 1716. ^{1}H NMR (400 MHz, $CDCl_3$, δ): 7.12–7.08 (m, 2H), 6.94–6.78 (m, 5H), 6.58–6.56 (m, 2H), 4.03–3.97 (m, 4H), 3.30–3.13 (m, 4H), 2.27 (t, J=5.5 Hz, 4H), 1.96 (d, J=3.7 Hz, 6H), 1.18 (t, J=7.1 Hz, 6H). ^{13}C NMR (100 MHz, $CDCl_3$, δ): 172.4, 150.0, 144.2, 136.7, 129.0, 128.6, 128.6, 125.8, 123.8, 123.5, 123.3, 121.5, 121.2, 120.9, 120.8, 119.9, 115.7, 102.0, 60.1, 48.8, 33.4, 18.7, 18.4, 14.1. HRMS (m/z): calcd 492.2386 (MH^+); found 492.2404.

4.1.9. 3,3′-Dimethyl-8-(iminodipropanoic acid)-2,2′-spirobi[2H-1-benzopyran] (**10b**)

To a solution of compound **9b** (49 mg, 0.0231 mmol) in THF (1 mL) in a 5 mL flask was added 40 μL of 4 N NaOH (0.09 mmol). The reaction mixture was stirred at room temperature and monitored with reverse-phase TLC (25% CH_3CN in water). Distilled water was added throughout 120 h of the reaction. The sample was lyophilized. The crude sample was then acidified with 6 M HCl and dissolved in a minimum of acetonitrile before being applied to a 6 mL SPE tube (Supelco Supelclean™ LC-18). Stepwise gradient elution using 10%, 20%, 30%, and 40% acetonitrile in water was used to isolate the pure product **10b** (19.2 mg, 45%). IR (KBr pallet, ν/cm^{-1}): 3426, 2600, 1716. ^{1}H NMR (400 MHz, CD_3CN, δ): 7.20–7.13 (m, 2H), 7.04–6.95 (m, 4H), 6.74–6.69 (m, 3H), 3.22–3.20 (m, 4H),

2.20 (t, J=6.8 Hz, 4H), 1.94 (d, J=0.8 Hz, 6H). ^{13}C NMR (400 MHz, CD_3CN, δ): 172.3, 149.6, 144.6, 134.7, 128.9, 126.1, 123.8, 123.5, 123.2, 122.9, 121.9, 121.7, 121.2, 119.8, 115.3, 102.2, 48.7, 31.1, 17.7, 17.5. HRMS (m/z): calcd 437.1760 (MH^+); found 436.1776.

*4.1.10. 2,3-Dihydro-2-oxobenzomorpholine-4-acetic acid (**11**)*

To a 500 mL 3-neck round bottom flask equipped with a condenser, 2-aminophenol (5.4 g, 0.049 mol), chloroacetic acid (9.8 g, 0.1 mol), sodium hydroxide (6 g, 0.15 mol), and 100 mL water were added. The reaction apparatus was evacuated and filled with N_2 (g). A solution of NaOH (6 M, aq) was added dropwise to the reaction until a pH of 8 was reached. The reaction mixture was refluxed for 3 h and pH was maintained at pH 7–8. The reaction mixture was cooled and concentrated HCl was added until the pH of the solution was strongly acidic. Solid brown deposits were filtered and redissolved in water. Charcoal was added and boiled for 5 min, filtered hot, and the filtrate was concentrated to ~100 mL. Overnight standing resulted in a white solid deposit in the bottom of the flask, which was filtered to give the desired compound **11** (6.73 g, 66%). IR (KBr pallet, ν/cm^{-1}): 3113, 1769, 1724, 1704. ^{1}H NMR (300 MHz, acetone-d_6, δ): 7.10–7.02 (m, 4H), 4.21 (d, J=4.8 Hz, 4H). ^{13}C NMR (75 MHz, acetone-d_6, δ): 171.0, 165.0, 142.7, 135.2, 125.8, 120.6, 117.3, 113.8, 51.1, 50.4. HRMS (m/z): calcd 207.0532; found 207.0526.

*4.1.11. Sodium (2-hydroxyphenyl)iminodiacetate (**12a**)*

A saturated solution of **11** was prepared in 10 mM Tris buffer pH 8.7. Conversion to **12a** occurred immediately according to ^{1}H NMR. ^{1}H NMR (300 MHz, Tris-d_{11}, 10 mM in D_2O, δ): 7.06 (d, J=7.5 Hz, 1H), 6.97 (t, J=7.5 Hz, 1H), 6.87–6.82 (m, 2H), 3.68 (s, 4H). ^{13}C NMR (75 MHz, Tris-d_{11}, 10 mM in D_2O, δ): 180.1, 149.9, 139.4, 124.3, 121.9, 120.9, 116.4, 113.5, 57.7.

*4.1.12. 2-Hydroxyphenyl iminodipropanoic acid (**12b**)*

To a 150 mL three-neck round bottom flask equipped with a condenser, 2-aminophenol (2.524 g, 2.31 mmol), 3-bromopropionic acid (14.313 g, 9.36 mmol), and 25 mL of H_2O were added. The reaction apparatus was evacuated and filled with N_2 (g). A 6 M solution of NaOH was added dropwise to the reaction until a pH of 8 was reached. The reaction mixture was refluxed for 3 h and pH was maintained at pH 7–8. Concentrated HCl was added until pH=4. The reaction mixture was extracted with ethyl acetate. The aqueous layer was then collected, reduced by boiling, and allowed to cool. A solid crystallized, which was purified by recrystallization with H_2O to give pure **12b** (0.20 g, 4%). IR (KBr pallet, ν/cm^{-1}): 2569, 1706. ^{1}H NMR (300 MHz, NaOD/D_2O, δ): 7.16–7.08 (m, 2H), 6.84–6.80 (m, 2H), 3.40 (t, J=6.3 Hz, 4H), 2.14 (t, J=6.3 Hz, 4H). ^{13}C NMR (100 MHz, D_2O/NaOD, δ): 179.2, 151.5, 129.4, 123.3, 120.5, 116.6, 53.0, 32.8. HRMS (m/z): calcd 253.0950; found 253.0958.

4.2. Binding study procedure (NMR)

Stock solutions of metals were made up using 2.00 mL volumetric flasks; [metal]=0.01–1.0 M in 10 mM HEPES buffer pH 9.8. Concentration of chelator was determined through integration of NMR signals (5 s delay) versus an internal integration and chemical shift standard 3-(trimethylsilyl)-1-propanesulfonic acid sodium salt (DSS). Binding constants were determined by performing ^{1}H NMR titrations of metal chloride (0–0.42 M in 10 mM HEPES-d_{18} pH 9.8) added to chelator (9.2×10^{-5} to 6.9×10^{-4} M in 10 mM HEPES-d_{18} pH 9.8). Spectra were taken on a Bruker DRX 400 MHz NMR or Bruker Avance 600 MHz spectrometer with a 5-mm inverse probe. The chemical shifts of three protons of the chelator (aromatic and aliphatic) for 10–14 different metal to chelator concentration ratios were determined. These data were collected and three independent binding studies for each metal chloride were fit to 1:1, 1:2, and 2:1 binding models in an iterative least-squares refinement procedure found in the Pascal program NMRspec. This program, written by Richard E. Barrans, Jr., generates association constants, the chemical shifts of the bound chelator for the binding model specified ($\Delta\delta_{max}$).

All NMR titrations were under fast exchange except for titration of **12a** with Mg^{2+}. For **12a**, a weighted average of two signals was calculated using integral value and peak position. This weighed average was input into NMRspec.

4.3. Binding study procedure (luminescence)

Stock solutions of compounds **1a**, **1b**, **10a**, and **10b** in the concentration range of 2.88×10^{-3} M to 2.1×10^{-4} M were prepared in 10 mM HEPES buffer pH 9.8 in 2 mL volumetric flasks. Metal chloride solutions (0.1–0.01 M) were prepared in 10 mM HEPES buffer pH 9.8 in 25 mL volumetric flasks by dilution of stock solutions of metal chloride (~1 M) in distilled water. The concentration of the buffered stock solution of chelator was determined by ^{1}H NMR integration versus the standard DSS. Luminescence data were obtained using two different luminescence spectrophotometers, using 10 mm path length cells. Spectra were background corrected for pure solvent, without degassing. For **1b**, 315 nm excitation was used, and the slit width for excitation and emission was 10 nm. For **10b**, 310 nm excitation was used, and the slit width for excitation and emission was 3 nm. The change in luminescence intensity of chelator (~1×10^{-5} to 3.27×10^{-5} M) with increasing concentration of metal chloride in 10 mM HEPES at pH 9.8 was recorded. Usually 12–17 additions were performed. The data were analyzed using the program Hyperquad 2000 written by Dr. Peter Gans, University of Leeds.

4.4. Quantum yield determinations

Quantum yields were determined by a procedure reported in the literature.[9a,b] The quantum yield was determined using the following equation:

$$\Phi_{\text{sample}} = \frac{F_{\text{sample}}}{F_{\text{anthracene}}} \times \frac{A_{\text{anthracene}}}{A_{\text{sample}}} \times \frac{n_s}{n_e} \times \Phi_{\text{anthracene}}$$

where F_{sample} and $F_{\text{anthracene}}$ are the measured area under the luminescence spectrum of sample and the anthracene, respectively. $A_{\text{anthracene}}$ and A_{sample} are the absorbances at 310 nm (or 315 nm) of the reference (anthracene) and sample in ethanol or HEPES buffer pH 9.8; η_s is the index of refraction of solvent in which sample was dissolved (1.3240 for methanol and 1.33156 for 10 mM HEPES buffer[14]) and η_e is the index of refraction of ethanol (1.3600); $\varphi_{\text{anthracene}}$ is the quantum yield of anthracence and assumed to be 1 at excitation wavelength 310 nm used for studies; 5 nm slit width was used during quantum yield measurements.

Acknowledgements

This work was supported by a generous grant from the National Institutes of Health (NIGMS MBRS S06 GM08101). Partial support for instrumentation is from the RIMI Program at California State University, Los Angeles (NIH-NCMHDP20-MD001824-01). Authors are thankful to Dr. M. Selke, Dr. N. C. Maiti, Dr. M. Piyasena, and Dr. L. Shi for helpful discussions; to Dr. F. Zhou and Dr. F. Gomez for providing access to fluorometers; to D. C. Hernandez for assistance with experiments.

Supplementary data

Compound characterization spectra; luminescence spectra discussed in the text; binding titration results for **1b** (^{1}H NMR) and **10b** (luminescence); sample output of Hyperquad program.

Supplementary data associated with this article can be found in the online version, at doi:10.1016/j.tet.2008.05.083.

References and notes

1. (a) Berridge, M. J.; Bootman, M. D.; Roderick, H. L. *Nat. Rev. Mol. Cell Biol.* **2003**, *4*, 517–529; (b) Carafoli, E. *Trends Biochem. Sci.* **2004**, *29*, 371–379; (c) Rizzuto, R.; Pozzan, T. *Physiol. Rev.* **2006**, *86*, 369–408; (d) Koninck, P. D.; Schulman, H. *Science* **1998**, *279*, 227–230.
2. (a) Furuta, T.; Noguchi, K. *Trends Anal. Chem.* **2004**, *23*, 511–519; (b) Momotake, A.; Lindegger, N.; Niggli, E.; Barsotti, R. J.; Ellis-Davies, G. C. R. *Nat. Methods* **2006**, *3*, 35–40; (c) Gurney, A. M.; Bates, S. E. *Meth. Neurosci.* **1995**, *27*, 123–152; (d) Davis, J. P.; Tikunova, S. B.; Walsh, M. P.; Johnson, J. D. *Biochemistry* **1999**, *38*, 4235–4244; (e) Tompa, P.; Töth-Boconádi, R.; Friedrich, P. *Cell Calcium* **2001**, *29*, 161–170.
3. (a) Fedorova, O. A.; Strokach, Y. P.; Chebuńkova, A. V.; Valova, T. M.; Gromov, S. P.; Alfimov, M. V.; Lokshin, V.; Samat, A. *Russ. Chem. Bull. Int. Ed.* **2006**, *55*, 287–294; (b) Roxburgh, C. J.; Sammes, P. G. *Eur. J. Org. Chem.* **2006**, 1050–1056; (c) Filley, J.; Ibrahim, M. A.; Nimlos, M. R.; Watt, A. S.; Blake, D. M. *J. Photochem. Photobiol., A* **1998**, *117*, 193–198; (d) Momotake, A.; Arai, T. *Tetrahedron Lett.* **2003**, *44*, 7277–7280; (e) Tanaka, M.; Kamada, K.; Ando, H.; Kitagaki, T.; Shibutani, Y.; Kimura, K. *J. Org. Chem.* **2000**, *65*, 4342–4347; (f) Kimura, K.; Sakamoto, H.; Nakamura, M. *Bull. Chem. Soc. Jpn.* **2003**, *76*, 225–245; (g) Ahmed, S. A.; Tanaka, M.; Hisanori, A.; Iwamotob, H.; Kimura, K. *Tetrahedron* **2004**, *60*, 3211–3220; (h) Ushakov, E. N.; Nazarov, V. B.; Fedorova, O. A.; Gromov, S. P.; Chebuńkova, A. V.; Alfimov, M. V.; Barigelletti, F. *J. Phys. Org. Chem.* **2003**, *16*, 306–309; (i) Liu, Z.; Jianga, L.; Lianga, Z.; Gao, Y. *J. Mol. Struct.* **2005**, *737*, 267–270; (j) Ohshima, A.; Momotake, A.; Arai, T. *Sci. Technol. Adv. Mater.* **2005**, *6*, 633–643; (k) Strokach, Y. P.; Valova, T. M.; Barachevskii, V. A.; Shienok, A. I.; Marevtsev, V. S. *Russ. Chem. Bull. Int. Ed.* **2005**, *54*, 1477–1480; (l) Kőszegi, E.; Grün, A.; Bitter, I. *Supramol. Chem.* **2006**, *18*, 67–76; (m) Sakata, T.; Jackson, D. K.; Mao, S.; Marriott, G. *J. Org. Chem.* **2008**, *73*, 227–233.
4. Lu, N. T.; Nguyen, V. N.; Kumar, S.; McCurdy, A. *J. Org. Chem.* **2005**, *70*, 9067–9070.
5. McCurdy, A. M.; Kawaoka, A. M.; Holly, T.; Yoon, S. C. *Tetrahedron Lett.* **2001**, *42*, 7763–7766.
6. Irving, H.; Da Silva, J. J. R. F. *J. Chem. Soc.* **1963**, 3308–3320.
7. Connors, K. A. *Binding Constants: The Measurement of Molecular Complex Stability*; Wiley: New York, NY, 1987.
8. Martell, A. E.; Hancock, R. D. *Metal Complexes in Aqueous Solutions*; Plenum: New York, NY, 1996.
9. (a) Eaton, D. F. *Pure Appl. Chem.* **1988**, *60*, 1107–1114; (b) Zhang, D.; Dufek, E. J.; Clennan, E. L. *J. Org. Chem.* **2006**, *71*, 315–319; (c) Parker, C. A. *Photoluminescence of Solutions*; Elsevier: New York, NY, 1968; pp 261–268; (d) Valeur, B. *Molecular Fluorescence*; Wiley-VCH: New York, NY, 2002; pp 159–161.
10. (a) Voloshin, N. A.; Chernyshev, A. V.; Metelitsa, A. V.; Besugliy, S. O.; Voloshina, E. N.; Sadimenko, L. P.; Minkin, V. I. *Arkivoc* **2004**, *xi*, 16–24; (b) Atabekyan, L. S.; Chibisov, L. S. *High Energy Chem.* **1996**, *30*, 261–266.
11. McFarland, S. A.; Finney, N. S. *J. Am. Chem. Soc.* **2001**, *123*, 1260–1261.
12. (a) Gans, P.; Sabatini, A.; Vacca, A. *Talanta* **1996**, *43*, 1739–1753; (b) Fedorov, Y. V.; Fedorova, O.; Schepel, N.; Alfimov, M.; Turek, A. M.; Saltiel, J. *J. Phys. Chem. A* **2005**, *109*, 8653–8660.
13. Christensen, T.; Gooden, D. M.; Kung, J. E.; Toone, E. J. *J. Am. Chem. Soc.* **2003**, *125*, 7357–7366.
14. Vörös, J. *Biophys. J.* **2004**, *87*, 553–561.